Identification of three LRR-RKs involved in perception of root meristem growth factor in *Arabidopsis*

Hidefumi Shinohara[a], Ayaka Mori[b], Naoko Yasue[c], Kumiko Sumida[c], and Yoshikatsu Matsubayashi[a,1]

[a]Division of Biological Science, Graduate School of Science, Nagoya University, Chikusa, Nagoya 464-8602, Japan; [b]Graduate School of Bio-Agricultural Sciences, Nagoya University, Chikusa, Nagoya 464-8601, Japan; and [c]National Institute for Basic Biology, Myodaiji, Okazaki 444-8585, Japan

Edited by Philip N. Benfey, Duke University, Durham, NC, and approved February 26, 2016 (received for review November 16, 2015)

A peptide hormone, root meristem growth factor (RGF), regulates root meristem development through the PLETHORA (PLT) stem cell transcription factor pathway, but it remains to be uncovered how extracellular RGF signals are transduced to the nucleus. Here we identified, using a combination of a custom-made receptor kinase (RK) expression library and exhaustive photoaffinity labeling, three leucine-rich repeat RKs (LRR-RKs) that directly interact with RGF peptides in *Arabidopsis*. These three LRR-RKs, which we named RGFR1, RGFR2, and RGFR3, are expressed in root tissues including the proximal meristem, the elongation zone, and the differentiation zone. The triple *rgfr* mutant was insensitive to externally applied RGF peptide and displayed a short root phenotype accompanied by a considerable decrease in meristematic cell number. In addition, PLT1 and PLT2 protein gradients, observed as a gradual gradient decreasing toward the elongation zone from the stem cell area in wild type, steeply declined at the root tip in the triple mutant. Because RGF peptides have been shown to create a diffusion-based concentration gradient extending from the stem cell area, our results strongly suggest that RGFRs mediate the transformation of an RGF peptide gradient into a PLT protein gradient in the proximal meristem, thereby acting as key regulators of root meristem development.

peptide hormone | receptor | plant | stem cell | sulfated peptide

Receptor kinases (RKs) constitute the largest family of cell surface transmembrane receptors in plants, representing 610 members in *Arabidopsis* (1). RKs have been shown to play a role in a wide variety of signal transduction pathways related to plant growth, development, environmental adaptation, and defense responses (2). In particular, there is a growing awareness that RKs regulate primary and secondary meristem development in response to binding of specific peptide ligands. These include CLAVATA1 (CLV1) and BARELY ANY MERISTEM1 (BAM1), which directly bind CLV3 peptide, involved in control of the stem cell population in the shoot apical meristem (3–5); TDIF RECEPTOR (TDR)/PHLOEM INTERCALATED WITH XYLEM (PXY), which interacts with TRACHEARY ELEMENT DIFFERENTIATION INHIBITORY FACTOR (TDIF)/CLAVATA3 ESR-related 41/44 (CLE41/44) peptides regulating vascular stem cell proliferation and differentiation (6); and CLV1 and ARABIDOPSIS CRINKLY4 (ACR4), which mediate CLE40 peptide signaling involved in stem cell differentiation in the distal meristem of the root cap (7). These findings highlight the importance of the RK-mediated peptide signaling pathway in controlling meristem development in plants (8), but it is still unknown whether RKs play roles in the regulation of proximal meristem activity in the root apical meristem (RAM).

An involvement of peptide signaling in proximal meristem development was initially suggested by phenotypic analysis of a loss-of-function mutant for tyrosylprotein sulfotransferase (TPST), which catalyzes posttranslational tyrosine sulfation of secreted peptides (9, 10). An *Arabidopsis* mutant deficient in TPST (*tpst-1*) shows a short-root phenotype characterized by a considerable decrease in proximal meristem cell number accompanied by reduced expression of stem cell transcription factors PLETHORA1 (PLT1) and PLT2. A subsequent search for sulfated peptides that rescue these meristem defects identified a 13-amino acid sulfated peptide, root meristem growth factor (RGF) (11). The RGF family of peptides comprises 11 genes in *Arabidopsis*, more than half of which are specifically expressed in quiescent center cells, columella stem cells, and the innermost layer of central columella cells in the root tip. Chemically synthesized RGF peptides restore meristem size by increasing meristematic cell number in the proximal meristem, accompanied by recovery of stem cell function in *tpst-1* roots (11). Conversely, *rgf1-1 rgf2-1 rgf3-1* triple mutation causes a short-root phenotype characterized by a decrease in meristematic cell number. RGF was later found to cause an irregular wavy growth pattern in roots when overexpressed and, although controversial (12), has been proposed to be involved in the gravitropic response (13).

RGF signaling targets PLT transcription factors, which define patterning of the root proximal meristem (11). PLT proteins display shootward gradient distributions that are highest in the stem cell area, with high levels of PLT maintaining stem cells, intermediate levels facilitating transit-amplifying cell divisions, and low levels allowing cellular differentiation (14). Because PLT1 and PLT2 protein expression and gradient dimensions are considerably reduced in *tpst-1* roots, but recover after the application of RGF peptide, RGF is proposed to be a key factor regulating proximal meristem activity through the PLT pathway (11).

Given that accumulating evidence indicates the critical importance of RGF signaling in proximal meristem development, RKs that can transduce extracellular RGF signals to nuclear PLT transcription factors should exist in the proximal meristem region. To this end, the present study aimed to identify membrane-localized RKs involved in RGF perception in *Arabidopsis*. Functional redundancy of this family, however, often makes it difficult to clearly discern the role of individual members by a genetic

Significance

There is a growing awareness that receptor kinases (RKs) regulate various aspects of plant development in response to perception of specific ligands, but the highly redundant nature of this family's members often makes it difficult to identify their ligands by a conventional mutant screening approach. To sidestep gene redundancy problems, here we used a combination of a custom-made RK expression library and exhaustive photoaffinity labeling and identified three RKs that directly interact with root meristem growth factor (RGF), a peptide hormone regulating root meristem development. The receptor triple mutant was insensitive to externally applied RGF peptide and displayed a short root phenotype accompanied by a considerable decrease in meristematic cell number, representing a previously unidentified ligand–receptor system in plants.

Author contributions: H.S. and Y.M. designed research; H.S., A.M., N.Y., K.S., and Y.M. performed research; H.S., A.M., N.Y., K.S., and Y.M. analyzed data; and H.S. and Y.M. wrote the paper.

The authors declare no conflict of interest.

This article is a PNAS Direct Submission.

[1]To whom correspondence should be addressed. Email: matsu@bio.nagoya-u.ac.jp.

This article contains supporting information online at www.pnas.org/lookup/suppl/doi:10.1073/pnas.1522639113/-/DCSupplemental.

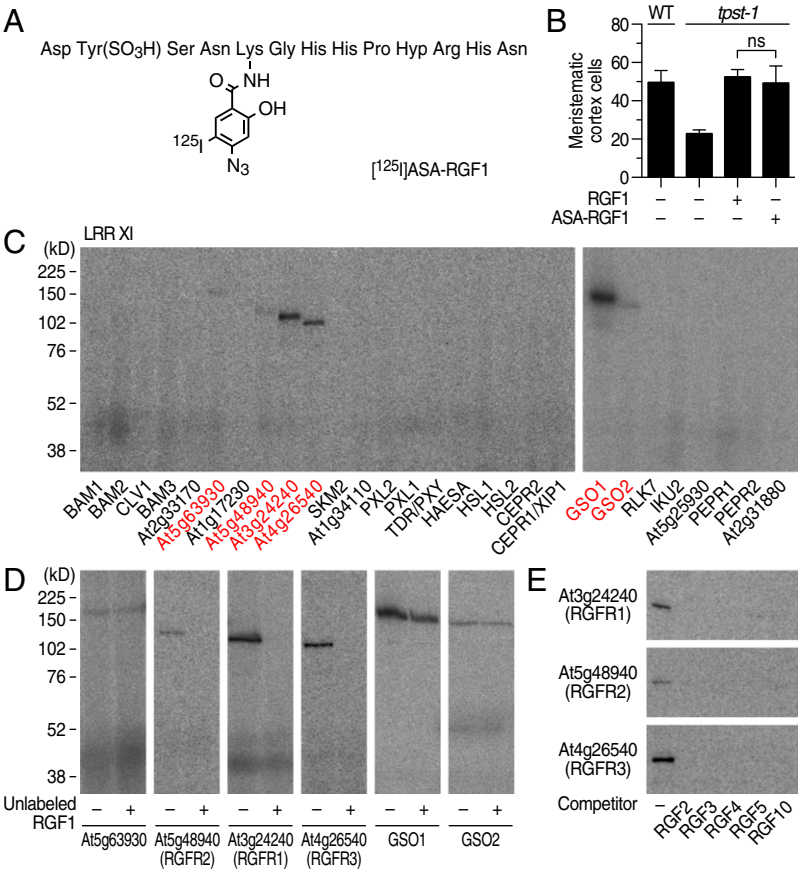

Fig. 1. Identification of three RKs that specifically interact with RGF by photoaffinity labeling. (*A*) Structure of [^{125}I]ASA-RGF1. (*B*) Biological activity of ASA-RGF1 determined by measuring meristematic cell number in the *tpst-1* mutant at 100 nM. Data represent mean values ± SD (n = 10–16; ns, not significant; paired t test). (*C*) Exhaustive photoaffinity labeling using [^{125}I]ASA-RGF1 against membrane fractions derived from individual RK expression lines. (*D*) Competitive displacement of [^{125}I]ASA-RGF1 binding by 300-fold excess unlabeled RGF1. (*E*) Competitive displacement of [^{125}I]ASA-RGF1 binding by 300-fold excess of other unlabeled RGF members.

approach. We thus used an exhaustive binding assay strategy taking advantage of a custom-made RK expression library, which allowed rapid identification of receptors without being hampered by their low abundance or gene redundancy. This approach enabled us to identify three leucine-rich repeat RKs (LRR-RKs) that redundantly act as specific receptors for RGF in the proximal meristem.

Results

Establishment of RK Expression Library. From the functional point of view, RKs can be divided into two groups; namely, ligand-binding receptors, which directly interact with ligands, and coreceptors, which form heteromers with ligand-binding receptors to modulate signaling. Cumulative evidence suggests the extracellular domain of ligand-binding receptors is quite large and mostly exceeds 400 amino acid residues (Dataset S1). In contrast, the size of typical coreceptors is so small that fewer than 300 amino acid residues have been found in the extracellular domain. In addition, genes encoding RKs that directly interact with small oligopeptide ligands contain no introns within the gene regions corresponding to the extracellular domain, with the only exception being the ERECTA family (15). Receptors for small ligands in plants might have evolved through gradual structural changes via point mutations, rather than the addition or swapping of domains. According to this empirical rule, we expected that RGF receptors should exist among the *Arabidopsis* RKs that have a large extracellular domain with no introns.

On the basis of this assumption, we analyzed the extracellular domain size of all the *Arabidopsis* RKs and found that 194 members carry an extracellular domain larger than 400 amino acid residues, including the N-terminal signal sequence. We excluded subfamilies to which members containing more than two introns belong, resulting in 95 members selected as primary candidates (Dataset S2). We individually overexpressed these RKs in tobacco BY-2 cells and established overexpression lines of 90 RKs (Fig. S1). No protein expression was detected for the remaining five RKs.

Identification of Three RGF Receptors by Exhaustive Photoaffinity Labeling. On the basis of the results from the alanine scanning experiments of RGF1 (Fig. S2*A*), we chemically synthesized a cross-linkable RGF1 derivative in which photoactivatable 4-azidosalicylic acid (ASA) is incorporated into the fifth residue from the N terminus. This ASA-RGF1 was radioiodinated to give [^{125}I]ASA-RGF1 (Fig. 1*A*). ASA-RGF1 retained biological activity comparable to that of unmodified RGF1 in stimulating meristematic cell division in the *tpst-1* mutant (Fig. 1*B*).

To identify RKs that directly interact with RGF1, we performed an exhaustive binding assay, using [^{125}I]ASA-RGF1 against membrane fractions derived from the 88 individual RK expression lines. Our binding assay used covalent photoaffinity labeling followed by immunoprecipitation of the target RKs to exclude false-positive bands arising from abundant proteases that potentially interact with peptide ligands. After SDS/PAGE and autoradiography, we detected binding of [^{125}I]ASA-RGF1 to six LRR-RKs, all of which belong to LRR-RK subfamily XI (Fig. 1*C*). Competitive displacement of bound [^{125}I]ASA-RGF1 by 300-fold excess unlabeled RGF1 confirmed that At3g24240, At5g48940, and At4g26540 specifically interact with RGF1 (Fig. 1*D*). These three LRR-RKs also interacted with RGF2, RGF3, RGF4, RGF5 [also known as GLV10 (16)], and RGF10 (At3g60650) peptides in a competitive manner with [^{125}I]ASA-RGF1, indicating that they recognize all the RAM-expressing RGF family peptides (Fig. 1*E*). Notably, RGF2, RGF3, RGF4, and RGF10 showed complete competition for binding of RGF1 to At3g24240 and At5g48940, even at low excess (10-fold) concentrations, indicating that these four RGF family peptides interact with affinities comparable to that of RGF1 (Fig. S2*B*). Functionally distinct

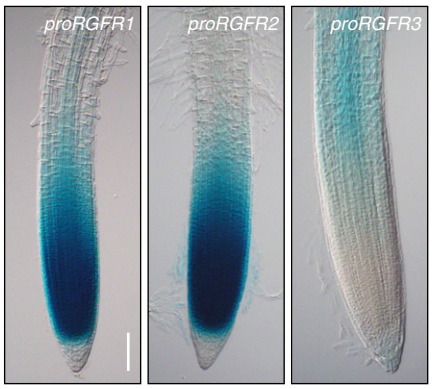

Fig. 2. Promoter activities of the *RGFR1*, *RGFR2*, and *RGFR3* genes. GUS activity is evident in the proximal meristem and the elongation zone of *proRGFR1:GUS* plants and *proRGFR2:GUS* plants, and in the elongation zone and differentiation zone of *proRGFR3:GUS* plants 5 d after germination (DAG). (Scale bar, 100 μm.)

peptide ligand CLV3 (3, 4), as a negative control, showed no binding to these three LRR-RKs, confirming ligand binding specificity of these LRR-RKs (Fig. S2*C*). In contrast, binding of [^{125}I] ASA-RGF1 to GSO1, GSO2, and At5g63930 was not competitively antagonized by excess unlabeled RGF1, indicating that the observed binding is nonspecific (Fig. 1*D*). We concluded that At3g24240, At5g48940, and At4g26540 are possible receptors for RGF and named them RGFR1, RGFR2, and RGFR3, respectively.

Promoter:GUS expression analysis in *Arabidopsis* plants revealed that promoter activity of *RGFR1* and *RGFR2* is predominantly observed in the proximal meristem, including the elongation zone, and gradually decreases toward the differentiation zone (Fig. 2). *RGFR2* (*At5g48940*) is also known as *ROOT CLAVATA-HOMOLOG1* (*RCH1*), the promoter of which has been used to express transgenes in root meristem (17). In contrast, *RGFR3* promoter activity is detected in the more basal region of the elongation zone and the differentiation zone. Public microarray data also support these tissue-specific *RGFR* expression patterns (18).

Phenotypic Analysis of *rgfr* Mutants. To analyze the effect of loss-of-function mutations of RGFRs on root meristem development, we identified T-DNA insertion mutants for each of the three *RGFR* genes (*rgfr1-1*, *rgfr2-1*, and *rgfr3-1*) (Fig. 3*A*). RT-PCR confirmed that a full-length transcript was absent in each mutant (Fig. S3*A*). The *rgfr1-1* single mutant showed a slight decrease in meristematic cell number in the RAM, whereas the *rgfr2-1* and *rgfr3-1* mutants were indistinguishable from the wild type (Fig. 3*B* and Fig. S3*B*). We further generated all combinations of double and triple knockout mutant plants to uncover possible redundant roles of RGFRs. We observed a considerable decrease in meristematic cell number in the *rgfr1-1 rgfr2-1 rgfr3-1* triple mutant to a level similar to that of the *tpst-1* mutant, which is deficient in biosynthesis of all sulfated peptides, including RGFs (Fig. 3 *B* and *C* and Fig. S3*B*) (9, 10). A substantial decrease in meristematic cell number was also found in the *rgfr1-1 rgfr2-1* double mutant, comparable to that in the *rgfr1-1 rgfr2-1 rgfr3-1* triple mutant, indicating a major role of RGFR1 and RGFR2 in regulating proximal meristem activity (Fig. 3*B* and Fig. S3*B*). Complementation of the *rgfr1-1 rgfr2-1* double mutant with RGFR1 genomic DNA reversed the double mutant phenotype, confirming that the observed morphological changes arise from the absence of functional RGFR proteins and validating the assumption of functional redundancy between RGFR1 and RGFR2 (Fig. 3*B* and Fig. S3*B*).

To examine whether the *rgfr1-1 rgfr2-1 rgfr3-1* triple mutant is defective in RGF responses, wild-type and mutant seedlings were cultured in a liquid medium containing 100 nM RGF1. Under the conditions in which wild-type roots respond to RGF1, the *rgfr1-1 rgfr2-1 rgfr3-1* triple mutant showed no detectable changes in meristematic cell number in the RAM (Fig. 3 *C* and *D*). Enhanced expansion and premature elongation of cells in the elongation zone, reminiscent of the phenotype conferred by *tpst-1* mutation, was also not alleviated by RGF1 treatment in the *rgfr1-1 rgfr2-1 rgfr3-1* triple mutant. Accordingly, the *rgfr1-1 rgfr2-1 rgfr3-1* triple mutant developed shorter roots than wild type because of the decrease in meristematic activity (Fig. 3 *E* and *F*).

The cell cycle marker *CYCB1;1-GUS* in the *rgfr1-1 rgfr2-1* double mutant indicated a reduction in cell division rate of the transit-amplifying zone and a decrease in the adjacent slow-dividing immature cell population zone that is thought to be a stem cell niche (Fig. 3*G*) (19). Importantly, the auxin distribution in *rgfr1-1 rgfr2-1* root tips visualized by the *DR5:GUS* marker was comparable to that of wild type, indicating that this root meristem defect is not associated with changes in auxin distribution (Fig. 3*H*).

In contrast to the evident role of the RGFRs in the proximal meristem, the *rgfr1-1 rgfr2-1 rgfr3-1* triple mutant displayed no obvious phenotype in the distal meristem (Fig. S3*C*). In addition, both public microarray data and our promoter activity analysis indicated no or low expression of these three *RGFR* genes in the distal meristem (Fig. 2) (18). Externally applied RGF has been shown to promote distal stem cell activity as well as proximal meristem activity in the *tpst-1* mutant (11). This might be interpreted as external RGF indirectly affecting distal stem cell activity as a result of recovery of proximal meristem function in *tpst-1*. Taken together, we concluded that RGFR1, RGFR2, and RGFR3 act as specific receptors for RGF peptides in the proximal meristem.

Loss of RGFRs Abolished PLT Protein Gradient in Proximal Meristem. PLT1 and PLT2 are AP2 class transcription factors that play a crucial role in root meristem development by mediating root stem cell niche patterning (14). PLT proteins show gradient expression patterns that extend from the stem cell area into the elongation zone across the region of rapidly dividing transit-amplifying cells. High PLT levels maintain stem cell identity, intermediate levels promote cell division of stem cell daughters, and low levels allow cell differentiation at the elongation zone (14). Because exogenous RGF application has been shown to cause enlargement of PLT1 and PLT2 expression domains (11), we investigated whether *rgfr1-1 rgfr2-1 rgfr3-1* triple mutation affects the PLT gradient in the RAM.

In wild-type plants, PLT1-GFP and PLT2-GFP exhibited a gradual shootward gradient from the root stem cell area (Fig. 4*A*). In contrast, gradients of PLT1-GFP and PLT2-GFP steeply declined at the root tip in the *rgfr1-1 rgfr2-1 rgfr3-1* background, with weak expression being retained in the stem cell area. In particular, the PLT2-GFP expression domain was strikingly diminished in the triple mutant compared with wild type (Fig. 4*A*). A similar reduction in the PLT2-GFP expression domain was also observed in the ligand triple mutant *rgf1-1 rgf2-1 rgf3-1*, albeit milder than in the receptor triple mutant, indicating that RGFs and RGFRs are required for maintaining a proper PLT gradient in the proximal meristem (Fig. 4*B*). Exogenous application of RGF1 to the ligand mutant *rgf1-1 rgf2-1 rgf3-1* caused drastic shootward enlargement of the PLT2-GFP expression domain to an even greater extent than the natural PLT2 gradient in wild type (Fig. 4*B*). This result can be interpreted as the intrinsic RGF peptide level defining the magnitude and the slope of the PLT gradient. In contrast, the receptor mutant *rgfr1-1 rgfr2-1 rgfr3-1* was substantially less sensitive to RGF1 with respect to recovery of PLT2-GFP expression (Fig. 4*C*). Collectively, these results indicate that the three RGFRs act as receptors for RGFs in the root meristem to define the PLT gradient.

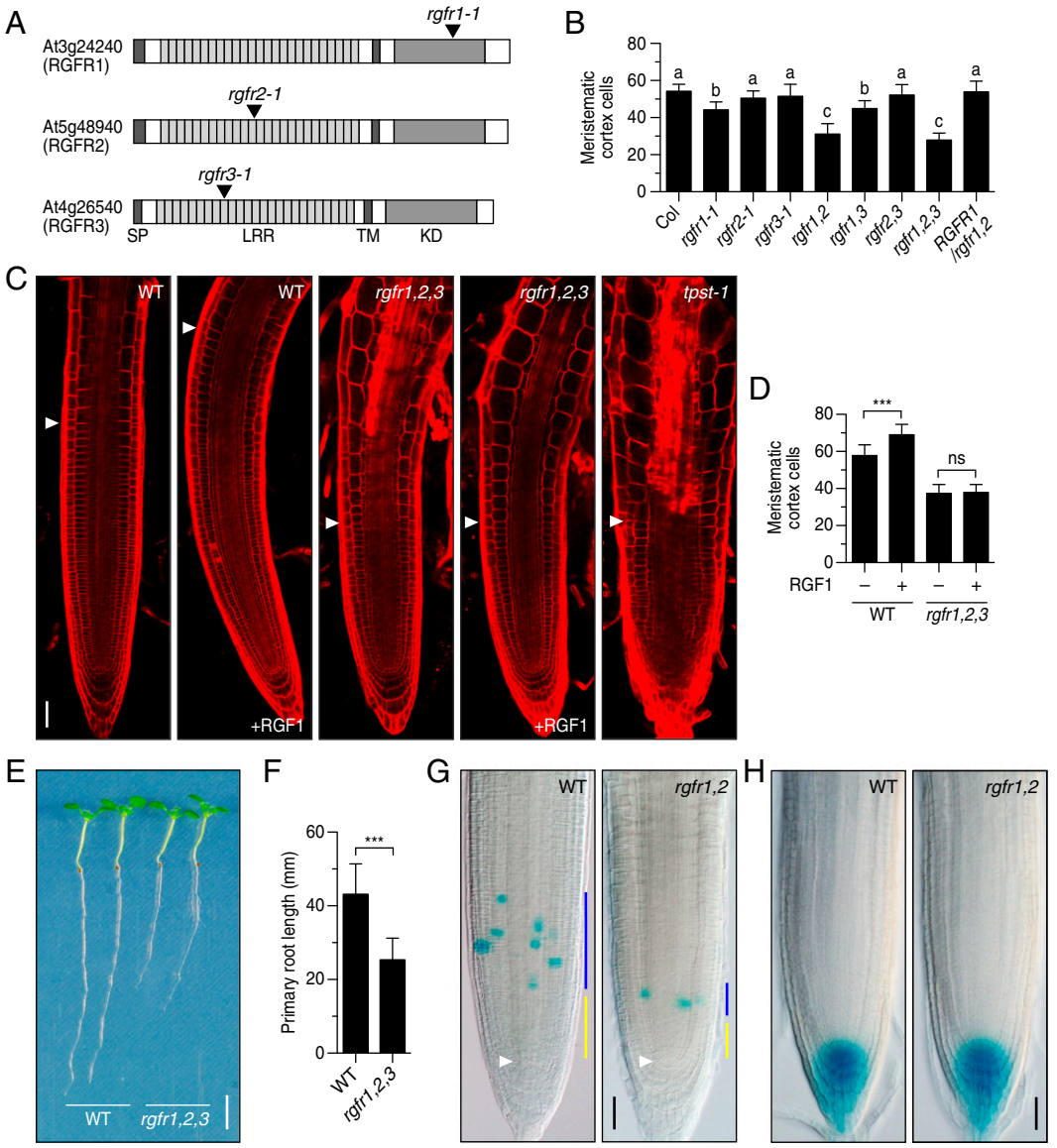

Fig. 3. Phenotypic analysis of T-DNA insertion mutants of the *RGFR* genes. (*A*) Schematic representation of T-DNA insertion sites in *rgfr1-1*, *rgfr2-1*, and *rgfr3-1*. (*B*) Number of meristematic cortex cells in root meristem of wild-type, *rgfr* mutants, and complemented line at 5 DAG. Significant differences are indicated with different letters (n = 16–23; one-way ANOVA, see also Fig. S3*B*). (*C*) Confocal images of root meristem of wild-type and *rgfr1-1 rgfr2-1 rgfr3-1* triple mutant treated with 100 nM RGF1 at 5 DAG. The root meristem of the *tpst-1* mutant is also shown as a reference. (*D*) Quantitative analysis of the number of meristematic cortex cells in Fig. 3*C* (n = 16–35; ***$P < 0.001$; paired t test). (*E*) Root length of wild-type and *rgfr1-1 rgfr2-1 rgfr3-1* triple mutant seedlings at 7 DAG. (*F*) Quantitative comparison of root length in Fig. 3*E* (n = 47–50; ***$P < 0.001$; paired t test). (*G*) *CYCB1;1-GUS* expression in wild type and *rgfr1-1 rgfr2-1* root meristem at 5 DAG. Blue bar represents transit amplifying zone; yellow bar represents slow-dividing immature cell population zone that is thought to be a stem cell niche. White arrowheads indicate the quiescent center. (*H*) *DR5:GUS* expression in wild type and *rgfr1-1 rgfr2-1* root meristems at 5 DAG. (Scale bar, *C*, *G*, and *H*, 50 μm; *E*, 5 mm.)

PLTs Are Very Proximal Downstream Targets of RGFRs. In contrast to the drastic changes in PLT2 protein expression patterns in the mutants, in situ hybridization showed that localization of *PLT2* transcripts was comparable among wild type, the *rgfr1-1 rgfr2-1 rgfr3-1* receptor mutant, and the *rgf1-1 rgf2-1 rgf3-1* ligand mutant, even after RGF1 treatment (Fig. 4*D* and Fig. S3*D*). In all lines, *PLT2* transcripts were detected only in the stem cell region, irrespective of the PLT2 protein distribution. These expression profiles suggest that RGF defines PLT expression patterns at the protein level, possibly through stabilization of PLT proteins.

We also analyzed the time course of changes in expression patterns of PLT2-GFP proteins in the *rgf1-1 rgf2-1 rgf3-1* ligand mutant after RGF1 treatment (Fig. 4*E*). Notably, the RGF response of the PLT2-GFP proteins was very rapid, and enlargement of PLT2-GFP expression domain was readily detected within 2–4 h after treatment. The PLT2-GFP expression domain further enlarged shootward to an even greater extent than in wild type after 12 h. These RGF response dynamics of PLT2-GFP proteins strongly suggest that PLTs are direct or very proximal downstream targets of RGFRs.

Discussion

We identified three LRR-RKs (RGFR1, RGFR2, and RGFR3) that specifically interact with RGF peptide by exhaustive photoaffinity labeling against a custom-made LRR-RK expression library. Multiple loss-of-function mutations in these LRR-RKs

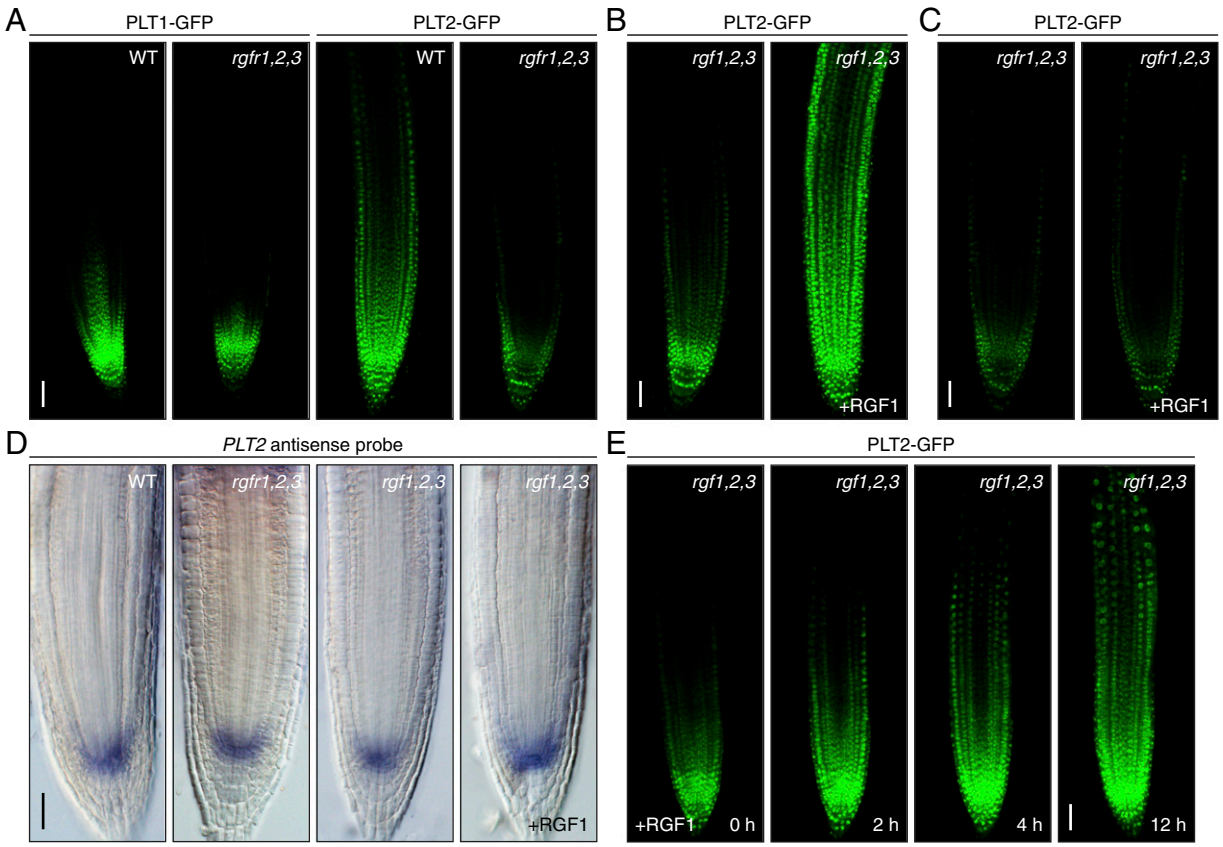

Fig. 4. RGFRs are required for maintaining proper gradients of PLT transcription factors in proximal meristem. (*A*) Confocal image of root meristem of wild-type and *rgfr1-1 rgfr2-1 rgfr3-1* receptor mutant seedlings expressing PLT1-GFP and PLT2-GFP at 5 DAG. (*B*) Root meristem of *rgf1-1 rgf2-1 rgf3-1* ligand mutant seedlings expressing PLT2-GFP treated with or without 100 nM RGF1 for 24 h. (*C*) Root meristem of *rgfr1-1 rgfr2-1 rgfr3-1* receptor mutant seedlings expressing PLT2-GFP treated with or without 100 nM RGF1 for 24 h. (*D*) Whole-mount in situ hybridization with *PLT2* antisense probe in root meristem of wild type, *rgfr1-1 rgfr2-1 rgfr3-1* receptor mutant, *rgf1-1 rgf2-1 rgf3-1* ligand mutant, and the ligand mutant treated with 100 nM RGF1 for 24 h. (*E*) Changes in expression patterns of PLT2-GFP proteins in *rgf1-1 rgf2-1 rgf3-1* ligand mutant after RGF1 treatment. (Scale bar, *A*–*E*, 50 μm.)

led to impaired RGF response and caused a short root phenotype characterized by a considerable decrease in meristematic cell number in the root proximal meristem. Competitive binding analysis revealed that the majority of the RAM-expressing RGF family peptides interact with RGFR1 and RGFR2 at affinities comparable that of RGF1, which indicates the potentially redundant action of these RGF family peptides. Competitive photoaffinity labeling, however, does not always precisely indicate the relative binding affinities of each peptide, especially when competitor peptides bind receptors at higher affinity than photoaffinity ligands. It has been recently reported that RGF1 and RGF2 play disparate roles in root development under phosphate depletion (20). One interpretation is that environmental stresses may affect expression levels and patterns of the three RGFR subtypes, which may have slightly different ligand recognition spectra.

We also found that RGFRs are required for maintaining proper gradients of PLT1 and PLT2 transcription factors, which regulate stem cell specification and transit-amplifying cell proliferation. In particular, PLT2 protein expression and gradient dimensions are considerably reduced both in the ligand mutant *rgf1-1 rgf2-1 rgf3-1* and the receptor mutant *rgfr1-1 rgfr2-1 rgfr3-1*. Importantly, exogenous application of RGF1 caused drastic enlargement of the PLT2-GFP expression domain in the ligand mutant, but not in the receptor mutant, to even greater levels than in wild type. Moreover, the RGF response of the PLT2-GFP proteins was very rapid, readily detectable within 2–4 h after treatment, suggesting that PLTs are direct or very proximal downstream targets of RGFRs. Because RGF peptides secreted from the stem cell region create a diffusion-based concentration gradient extending shootward from the stem cell area (11), our results strongly suggest that RGFRs mediate the transformation of an RGF peptide gradient into a PLT protein gradient in the proximal meristem, thereby acting as key regulators of root meristem development.

From the biochemical point of view, the slope of the gradient of RGF is defined exclusively by the half-life of RGF degradation and the diffusion coefficient of the peptides. Degradation mechanisms of the peptide hormones are not well understood, but major proteolytic activity in the apoplast is attributable to nonspecific proteases that degrade a broad spectrum of peptides at a certain rate (21). The diffusion coefficient is a physical parameter that is solely proportional to the molecular weight, and independent of environmental fluctuations. Thus, even though transcription of *RGF* genes is influenced by environmental changes, the gradient slope of RGF itself would remain largely stable. Under this system, a particular RGF concentration zone may shift spatially, depending on the *RGF* gene expression levels, but is always maintained somewhere within the gradient, which enables buffering of short-term environmental fluctuations. *PLT* gene expression is affected by auxin (14), whereas the PLT protein gradient has been shown not to be a readout of the auxin distribution but, rather, is suggested to be regulated at the level of protein stability (11, 19). Therefore, it is tempting to propose that a simple diffusion-based RGF peptide gradient defines the PLT protein gradient by modulating the stability of these proteins

to ensure robust root growth and development in fluctuating natural environments.

Materials and Methods

Expression of *Arabidopsis* Receptor Kinases in Tobacco BY-2 Cells. To overexpress *Arabidopsis* receptor kinases in tobacco BY-2 cells, we amplified the genomic fragment of each receptor kinase gene that corresponds from the Met[1] to the end of the juxtamembrane domain and the entire ORF of the HaloTag vector (Promega) by PCR. These two fragments were cloned in translational fusion by three-component ligation into the BamHI/SacI-digested binary vector pBI121, using an In-Fusion HD Cloning Kit (Clontech). Transformation of tobacco BY-2 cells and preparation of microsomal fractions were as described previously (4). Expressed HaloTag-fused receptors were specifically labeled using HaloTag TMR ligand (Promega), separated by SDS/PAGE, and visualized using a Typhoon 9400 fluorescent image analyzer (GE Healthcare) with a 523-nm excitation filter and a 580-nm emission filter.

Preparation of [^{125}I]ASA-RGF1 and Photoaffinity Labeling. The Fmoc-protected RGF1 analog Fmoc-[Lys^5]RGF1 was synthesized by Fmoc chemistry, using a peptide synthesizer (Applied Biosystems Model 431A). This peptide was reacted with 4-azidosalicylic acid succinimidyl ester (Pierce), followed by deprotection with piperidine to yield [(4-azidosalicyl)-Lys^5]RGF1 (ASA-RGF1). ASA-RGF1 was further radioiodinated by the chloramine T method, as previously described (4). The labeled peptide was purified by reverse-phase HPLC to yield analytically pure [^{125}I]ASA-RGF1 with specific radioactivity of 80 Ci/mmol. Photoaffinity labeling, immunoprecipitation, and SDS/PAGE were performed according to a previous report (22), using 30 nM [^{125}I]ASA-RGF1. Control binding experiments using [^{125}I]ASA-[Ara$_3$]CLV3 were performed as previously described (3).

Plant Materials and Growth Conditions. *Arabidopsis* ecotype Columbia (Col) was used. T-DNA–tagged *rgfr* mutants were identified in the SALK T-DNA collections (*rgfr1-1*, SALK_040393; *rgfr2-1*, SALK_096206; *rgfr3-1*, SALK_053167) (23). Marker line *CYCB1;1:GUS* was a gift from P. Doerner, University of Edinburgh, Edinburgh (24), and the *DR5:GUS* marker was from T. Guilfoyle, University of Missouri, Columbia, MO (25). For PLT1/PLT2 expression analysis in the *rgfr1 rgfr2 rgfr3* triple mutant, *rgfr* mutant lines were directly transformed with the *PLT1-GFP* and *PLT2-GFP* translational fusions (11), using the floral dipping method. For complementation analysis, a 5.8-kb genomic DNA fragment containing the entire ORF along with 2.5 kb upstream of the ATG start codon was amplified from Col genomic DNA. The PCR product was cloned into the pBI101-Hm vector, and the resulting construct was introduced into *rgfr1-1 rgfr2-1* double-mutant plants. For the analysis of root meristem and PLT1/PLT2-GFP expression, surface-sterilized *Arabidopsis* seeds were directly sown into 1.0 mL B5 medium containing 1.0% sucrose in 24-well microplates and vernalized for 2 d at 4 °C, then incubated without shaking under continuous light at 22 °C for 5–8 d. For the analysis of root length, plants were vertically grown on the same medium solidified with 1.5% agar. All plants were grown under continuous light at 22 °C. Peptides were added to the medium at 100 nM.

Promoter Analysis of *RGFR1*, *RGFR2*, and *RGFR3*. The 2.5-kb promoter regions upstream of *RGFR1*, *RGFR2*, and *RGFR3* (including the initiation codon) were amplified and cloned by translational fusion in-frame with the β-glucuronidase (GUS) coding sequence in the binary vector pBI101 and transformed into *Arabidopsis* wild type. For GUS staining, β-glucuronidase activity was visualized by X-Gluc as substrate, using a conventional protocol.

Microscopy and Histochemistry. For confocal root imaging, cell outlines were stained with 50 μg/mL propidium iodide for 2 min and observed under a confocal laser-scanning microscope (Olympus FV300) with helium-neon laser excitation at 543 nm. GFP images were collected after argon laser excitation at 488 nm. The number of root meristematic cells was obtained by counting cortex cells showing no signs of rapid elongation. For visualization of starch granules and cell walls in root tips, mPS-PI staining was performed according to a previous report (26). Whole-mount in situ hybridization experiments were performed as previously described (11).

ACKNOWLEDGMENTS. We thank Mari Ogawa-Ohnishi for technical assistance with whole-mount in situ hybridization. This research was supported by a Grant-in-Aid for Scientific Research (S) (25221105 to Y.M.), a Grant-in-Aid for Scientific Research on Innovative Areas (15H05957 to Y.M. and 26113520 to H.S.), and a Grant-in-Aid for Young Scientists (B) (25840111 to H.S.).

1. Shiu SH, Bleecker AB (2001) Receptor-like kinases from *Arabidopsis* form a monophyletic gene family related to animal receptor kinases. *Proc Natl Acad Sci USA* 98(19): 10763–10768.
2. Gish LA, Clark SE (2011) The RLK/Pelle family of kinases. *Plant J* 66(1):117–127.
3. Shinohara H, Matsubayashi Y (2015) Reevaluation of the CLV3-receptor interaction in the shoot apical meristem: Dissection of the CLV3 signaling pathway from a direct ligand-binding point of view. *Plant J* 82(2):328–336.
4. Ogawa M, Shinohara H, Sakagami Y, Matsubayashi Y (2008) *Arabidopsis* CLV3 peptide directly binds CLV1 ectodomain. *Science* 319(5861):294.
5. Guo Y, Han L, Hymes M, Denver R, Clark SE (2010) CLAVATA2 forms a distinct CLE-binding receptor complex regulating *Arabidopsis* stem cell specification. *Plant J* 63(6): 889–900.
6. Hirakawa Y, et al. (2008) Non-cell-autonomous control of vascular stem cell fate by a CLE peptide/receptor system. *Proc Natl Acad Sci USA* 105(39):15208–15213.
7. Stahl Y, et al. (2013) Moderation of *Arabidopsis* root stemness by CLAVATA1 and ARABIDOPSIS CRINKLY4 receptor kinase complexes. *Curr Biol* 23(5):362–371.
8. Matsubayashi Y (2014) Posttranslationally modified small-peptide signals in plants. *Annu Rev Plant Biol* 65:385–413.
9. Zhou W, et al. (2010) *Arabidopsis* Tyrosylprotein sulfotransferase acts in the auxin/PLETHORA pathway in regulating postembryonic maintenance of the root stem cell niche. *Plant Cell* 22(11):3692–3709.
10. Komori R, Amano Y, Ogawa-Ohnishi M, Matsubayashi Y (2009) Identification of tyrosylprotein sulfotransferase in *Arabidopsis*. *Proc Natl Acad Sci USA* 106(35): 15067–15072.
11. Matsuzaki Y, Ogawa-Ohnishi M, Mori A, Matsubayashi Y (2010) Secreted peptide signals required for maintenance of root stem cell niche in *Arabidopsis*. *Science* 329(5995):1065–1067.
12. Meng L, Buchanan BB, Feldman LJ, Luan S (2012) CLE-like (CLEL) peptides control the pattern of root growth and lateral root development in *Arabidopsis*. *Proc Natl Acad Sci USA* 109(5):1760–1765.
13. Whitford R, et al. (2012) GOLVEN secretory peptides regulate auxin carrier turnover during plant gravitropic responses. *Dev Cell* 22(3):678–685.
14. Galinha C, et al. (2007) PLETHORA proteins as dose-dependent master regulators of *Arabidopsis* root development. *Nature* 449(7165):1053–1057.
15. Lee JS, et al. (2015) Competitive binding of antagonistic peptides fine-tunes stomatal patterning. *Nature* 522(7557):439–443.
16. Fernandez A, et al. (2013) Transcriptional and functional classification of the GOLVEN/ROOT GROWTH FACTOR/CLE-like signaling peptides reveals their role in lateral root and hair formation. *Plant Physiol* 161(2):954–970.
17. Casamitjana-Martínez E, et al. (2003) Root-specific *CLE19* overexpression and the *sol1/2* suppressors implicate a CLV-like pathway in the control of *Arabidopsis* root meristem maintenance. *Curr Biol* 13(16):1435–1441.
18. Schmid M, et al. (2005) A gene expression map of *Arabidopsis thaliana* development. *Nat Genet* 37(5):501–506.
19. Mähönen AP, et al. (2014) PLETHORA gradient formation mechanism separates auxin responses. *Nature* 515(7525):125–129.
20. Cederholm HM, Benfey PN (2015) Distinct sensitivities to phosphate deprivation suggest that RGF peptides play disparate roles in *Arabidopsis thaliana* root development. *New Phytol* 207(3):683–691.
21. Delannoy M, et al. (2008) Identification of peptidases in *Nicotiana tabacum* leaf intercellular fluid. *Proteomics* 8(11):2285–2298.
22. Shinohara H, Moriyama Y, Ohyama K, Matsubayashi Y (2012) Biochemical mapping of a ligand-binding domain within *Arabidopsis* BAM1 reveals diversified ligand recognition mechanisms of plant LRR-RKs. *Plant J* 70(5):845–854.
23. Alonso JM, et al. (2003) Genome-wide insertional mutagenesis of *Arabidopsis thaliana*. *Science* 301(5633):653–657.
24. Colón-Carmona A, You R, Haimovitch-Gal T, Doerner P (1999) Technical advance: Spatio-temporal analysis of mitotic activity with a labile cyclin-GUS fusion protein. *Plant J* 20(4):503–508.
25. Ulmasov T, Murfett J, Hagen G, Guilfoyle TJ (1997) Aux/IAA proteins repress expression of reporter genes containing natural and highly active synthetic auxin response elements. *Plant Cell* 9(11):1963–1971.
26. Truernit E, et al. (2008) High-resolution whole-mount imaging of three-dimensional tissue organization and gene expression enables the study of Phloem development and structure in *Arabidopsis*. *Plant Cell* 20(6):1494–1503.